(Scion Corporation, USA).

Results

Figure 2 shows successive images obtained from CA after stenting (top), as well as the enhanced images (middle). To extract the vortex movement, after the post-processing of two images, two images at successive times were subtracted one by one (bottom). The subtracted images exhibit the fluid entering the aneurysm with sufficient image contrast. The fluid in the aneurysm was composed of an inflow zone at the distal neck and an outflow zone at the proximal neck. A rotating vortex was formed in the distal zone of the aneurysm in each systole phase. The vortex circulated along the aneurysm wall rotating on itself. As the vortex traveled, it grew in diameter and lost its cohesion. The fluid in the aneurysm was pushed out in the diastole phase and at the beginning of the following systole phase. After enhancement of these images, two images of successive times were subtracted one by one to extract the vortex movement and then the center of the vortex was traced to measure the movement distance. The slipstream line method was employed to compare and validate the images by contrast with CA. Figure 3 shows successive enhanced images of the slipstream line indicating vortex movement. The inflow and outflow zones and

the rotating direction of the vortex are the same as in the images from the CA with contrast.

Figure 4 shows a graph of movement distances depending on time of the vortexes without the stent after application of the SVC method. From Figure 5, which shows the distances with the stent, it can be seen that the contrast with CA corresponds with the slipstream line. Figures 4 and 5 show that the speed of movement was reduced after stenting.

Table 1 shows the flow speed after application of the SVC method from 0 to 0.4 seconds, respectively. The speed with CA was consistent with that with the slipstream line. The speed was reduced after stent placement.

Discussion

Flow speed in the aneurysm cavity is one of the most important parameters to evaluate circulation of the blood in a cerebral aneurysm, shear stress, and the functioning of medical devices.

The integration of the SVC method into medical imaging devices may allow not only medical engineers but also all clinical operators to use this method for analysis of the flow in aneurysms and evaluation of the influence of medical devices on blood speed. The results of contrast movements were consistent with those of the slipstream line, indicating the possibility of using the SVC method in the medical field.

The SVC we employed in our study consisted of several free or relatively inexpensive software packages, which means that many operators or technicians can easily adopt this system.

The contrast image was performed by CA, which is capable of imaging 25 fps. When compared with conventional frames per second such as 2 or 6 fps, CA can trace the vortex more smoothly and accurately (15).

The reduction in speed of vortex movement after stent placement in the

aneurysm was consistent with many previous results (7, 8, 12, 17, 19). Such reduction may lead to formation of a thrombus and allow repair of the aneurysm by occlusion.

Several drawbacks of application of the SVC method to medical images should be mentioned.

The tubular model, which was simplified with one straight parent artery and one simple aneurysm in this study, may induce a different flow pattern than that of a realistic model or that of an actual patient. However, since Barath performed the SVC method with a realistic model and the employed particles exhibited a rotating vortex along the aneurysm (17), it should be possible to apply and carry out this method with CA in a realistic model or patient if the vortex is detected.

The tubular model made of silicone may limit lateral displacements of the wall with the pulsatile flow because silicone has a lower compliance than a real vessel. The wall displacements may be larger when used with the Poly (vinyl alcohol) model developed by Ohta et al. (20) and may change the flow pattern.

Nitinol used for a self-expandable stent is hard to visualize with angiography, and with stent markers, only the position of a stent can be detected. Although the LEO stent (Balt, France) with highly radiopaque wires allowed greater visibility in

this study, the structure near the neck was invisible compared with the case of a coronary stainless steel stent (21).

The spatial resolution of DSA should be improved if contrast images are to be used as way of measuring flow speed. The resolution in this study was 0.36 mm/pixel and so there were only about around 28 pixels on the diameter of aneurysm. Micro- angiography may provide a good view around the neck of an aneurysm in perforated vessels (22).

Conclusion

To measure the blood flow speed in a cerebral aneurysm using DSA, the SVC method was applied to successive images of CA. The obtained successive images were clear, indicating the possibility of its use for evaluating the impact of stents on flow speed in cerebral aneurysms. The rotating vortex along the aneurismal wall was observed and its movement was consistent with the images of the slipstream line.

Acknowledgement

We are thankful to Mr. Jesper Thyregod (COOK-WCE) and Mr. Drazenko Babic

(Philips Medical Systems) for financial grants, Philips Medical Systems for mechanical techniques, Dr. Fabienne Betting for facilitating access to data in Geneva University Hospital, and Dr. Francis Cassot (INSERN, Toulouse) for his pioneering development of the SVC method

References

1. Fiorella D, Albuquerque FC, Han P, McDougall CG. Preliminary experience using the Neuroform stent for the treatment of cerebral aneurysms. Neurosurgery 2004; 54:6-16; discussion 16-17.
2. Howington JU, Hanel RA, Harrigan MR, Levy EI, Guterman LR, Hopkins LN. The Neuroform stent, the first microcatheter-delivered stent for use in the intracranial circulation. Neurosurgery 2004; 54:2-5.
3. Lopes D, Sani S. Histological postmortem study of an internal carotid artery aneurysm treated with the Neuroform stent. Neurosurgery 2005; 56:E416; discussion E416.
4. Lylyk P, Ferrario A, Pasbon B, Miranda C, Doroszuk G. Buenos Aires experience with the Neuroform self-expanding stent for the treatment of intracranial aneurysms. J Neurosurg 2005; 102:235-241.
5. Lieber BB, Livescu V, Hopkins LN, Wakhloo AK. Particle image velocimetry assessment of stent design influence on intra-aneurysmal flow. Ann Biomed Eng 2002; 30:768-777.
6. Rhee K, Han MH, Cha SH. Changes of flow characteristics by stenting in aneurysm models: influence of aneurysm geometry and stent porosity. Ann Biomed Eng 2002; 30:894-904.
7. Steiger HJ, Perktold K. Computer modeling of intracranial saccular and lateral aneurysms for the study of their hemodynamics. Neurosurgery 1997; 41:326-327.
8. Aenis M, Stancampiano AP, Wakhloo AK, Lieber BB. Modeling of flow in a straight stented and nonstented side wall aneurysm model. J Biomech Eng 1997; 119:206-212.
9. Hirabayashi M, Ohta M, Rufenacht DA, Chopard B. Characterization of flow

reduction properties in an aneurysm due to a stent. Phys Rev E Stat Nonlin Soft Matter Phys 2003; 68:021918.

10. Hirabayashi M, Ohta M, Rufenacht DA, Chopard B. A lattice Boltzmann study of blood flow in stented aneurysms. FGCS 2003.
11. Hamuro M, Palmaz JC, Sprague EA, Fuss C, Luo J. Influence of stent edge angle on endothelialization in an in vitro model. J Vasc Interv Radiol 2001; 12:607-611.
12. Ohta M, Hirabayashi M, Wetzel S, et al. Impact of stent design on intra-aneurysmal flow: A computer simulation study. Interventional Neuroradiology 2004; 10:85-94.
13. Isoda H, Ramsey RG, Takehara Y, Takahashi M, Kaneko M. MR angiography of aneurysm models of various shapes and neck sizes. AJNR Am J Neuroradiol 1997; 18:1463-1472.
14. Wakhloo AK, Lieber BB, Rudin S, Fronckowiak MD, Mericle RA, Hopkins LN. A novel approach to flow quantification in brain arteriovenous malformations prior to enbucrilate embolization: use of insoluble contrast (Ethiodol droplet) angiography. J Neurosurg 1998; 89:395-404.
15. Sadasivan C, Lieber BB, Gounis MJ, Lopes DK, Hopkins LN. Angiographic quantification of contrast medium washout from cerebral aneurysms after stent placement. AJNR Am J Neuroradiol 2002; 23:1214-1221.
16. Asakura F, Tenjin H, Sugawa N, Kimura S, Oki F. Evaluation of intra-aneurysmal blood flow by digital subtraction angiography: blood flow change after coil embolization. Surg Neurol 2003; 59:310-319; discussion 319.
17. Barath K, Cassot F, Rufenacht DA, Fasel JH. Anatomically shaped internal carotid artery aneurysm in vitro model for flow analysis to evaluate stent effect. AJNR Am J Neuroradiol 2004; 25:1750-1759.
18. Barath K, Cassot F, Fasel JH, Ohta M, Rufenacht DA. Influence of stent properties on the alteration of cerebral intra-aneurysmal haemodynamics: flow quantification in elastic sidewall aneurysm models. Neurol Res 2005; 27 Suppl 1:S120-128.
19. Yu SC, Zhao JB. A steady flow analysis on the stented and non-stented sidewall aneurysm models. Med Eng Phys 1999; 21:133-141.
20. Ohta M, Handa A, Iwata H, Rufenacht DA, Tsutsumi S. Poly-vinyl alcohol hydrogel vascular models for in vitro aneurysm simulations: the key to low friction surfaces. Technol Health Care 2004; 12:225-233.
21. Rudin S, Wu Y, Kyprianou I, et al. Micro-angiographic detector with fluoroscopic capability. In: Larry E. Antonuk MJY, Editors,, ed. Medical Imaging 2002: Physics of Medical Imaging, Proceedings of SPIE, 2002; 344-354.
22. Rudin S, Wang Z, Kyprianou I, et al. Measurement of Flow Modification in Phantom

Aneurysm Model: Comparison of Coils and a Longitudinally and Axially Asymmetric Stent–Initial Findings. Radiology 2004; 231:272-276.

Figure captions

Figure 1 Transparent silicone model of an aneurysm with a 5 mm neck and a diameter of 10 mm on a straight parent artery with a diameter of 3.5 mm.

Figure 2 Successive images obtained from CA and the post-processing of the images. The top shows raw images, the middle presents an enhanced images and the bottom shows subtracted images.

Figure 3 Successive images obtained from a slipstream line and the post-processing of the images. The top shows raw images and the bottom presents subtracted images.

Figure 4 Graph of movement distances depending on time of the vortexes without the stent application of the SVC method for comparison between CA and slipstream line.

Figure 5 Graph of movement distances depending on time of the vortexes with the stent after application of the SVC method for comparison between CA and slipstream line. The flow speeds are reduced after the stenting when compared with Figure 4.

Table 1 List of flow speeds after application of the SVC method from 0 to 0.4 second

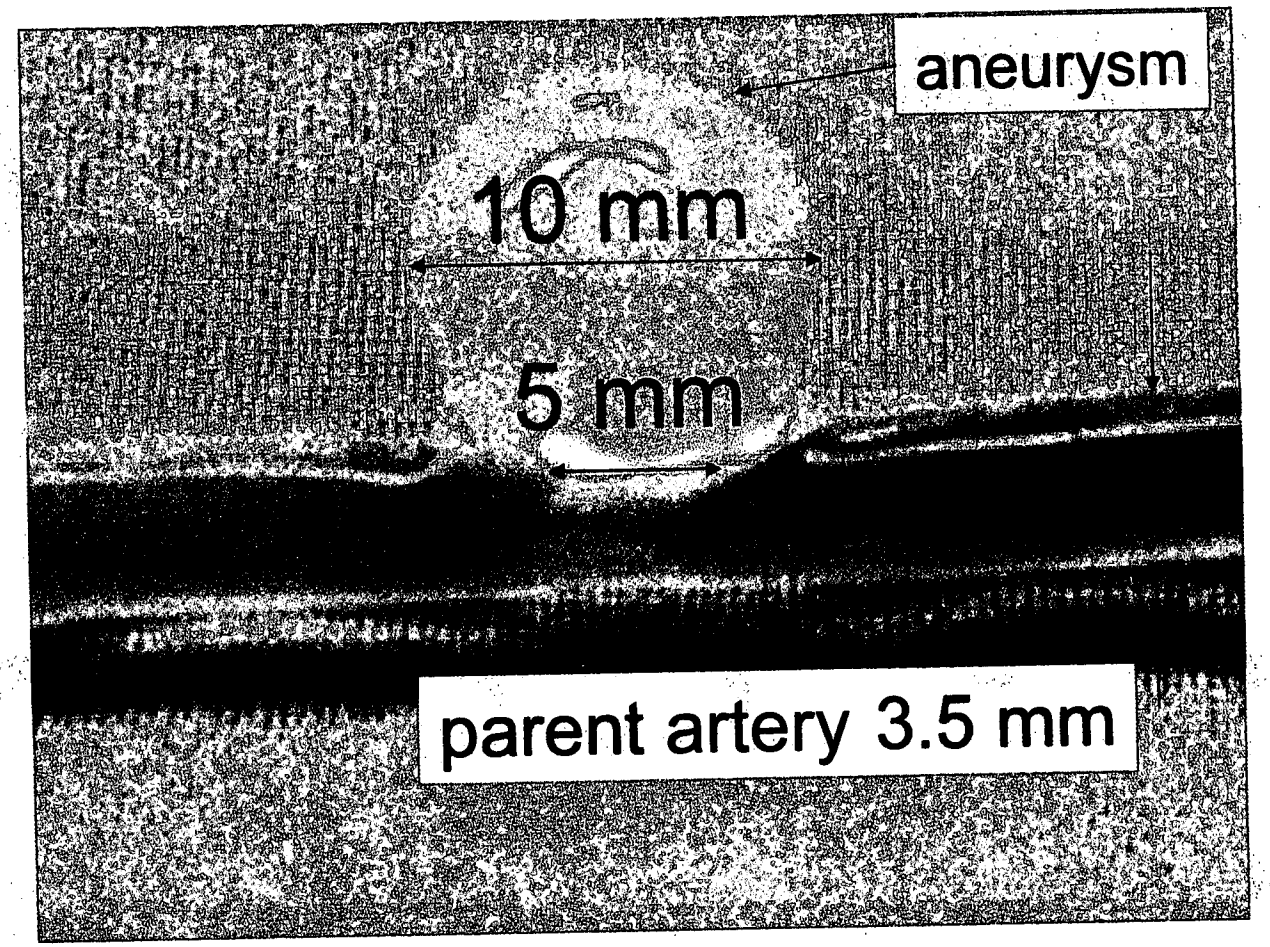

Fig. 1

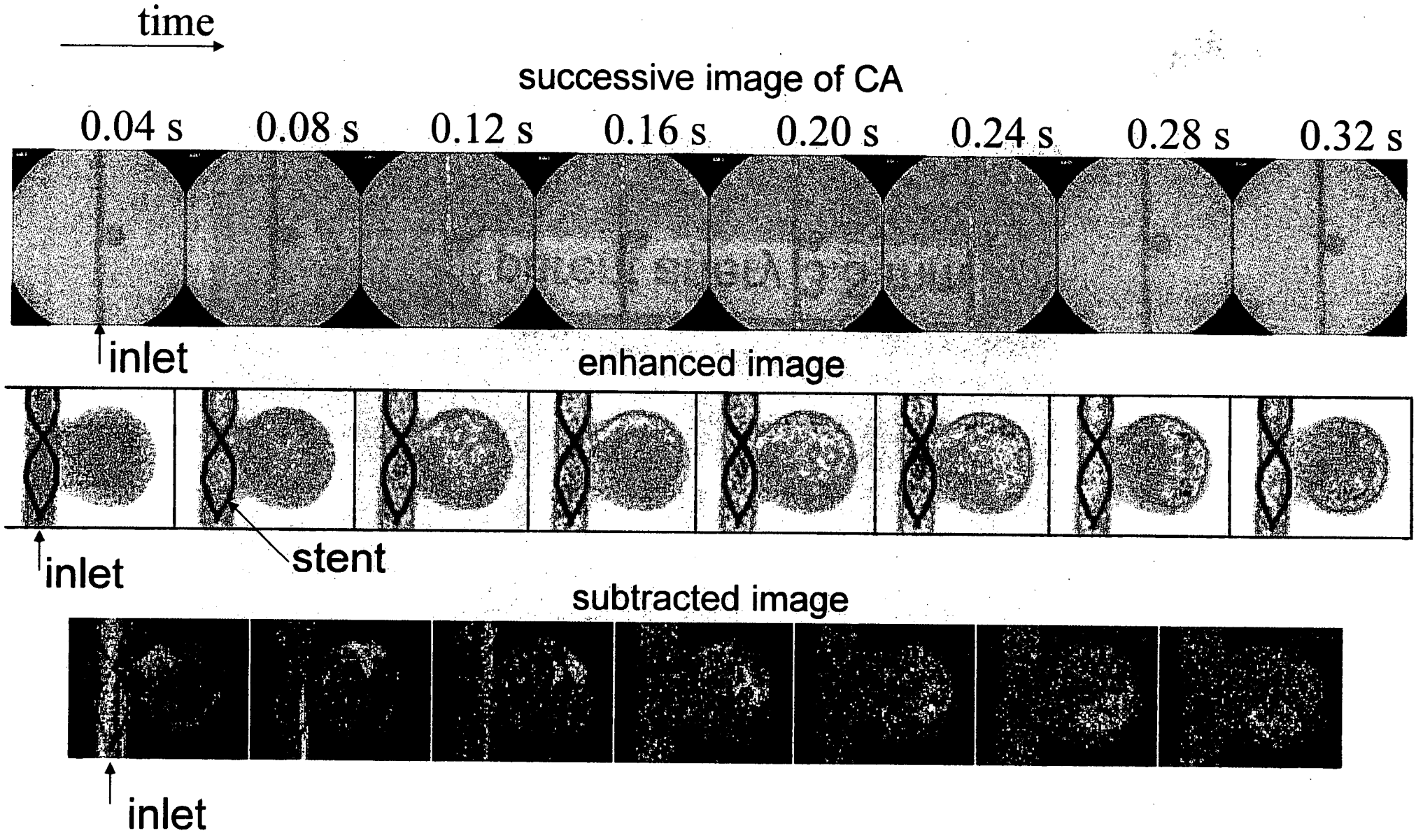
time
successive image of CA
0.04 s
0.08 s
0.12 s
0.16 s
0.20 s
0.24 s
0.28 s
0.32 s
inlet
enhanced image
inlet
stent
subtracted image
inlet

Fig. 2


successive image of slipstream line
1/30 s
2/30 s
3/30 s
4/30 s
5/30 s
6/30 s
7/30 s
8/30 s
9/30 s
10/30 s
inlet
stent

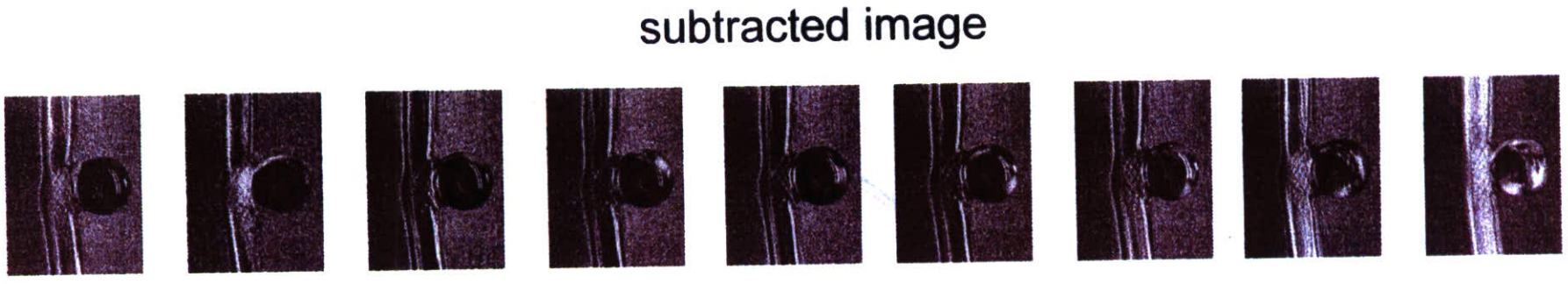
subtracted image

Fig. 3

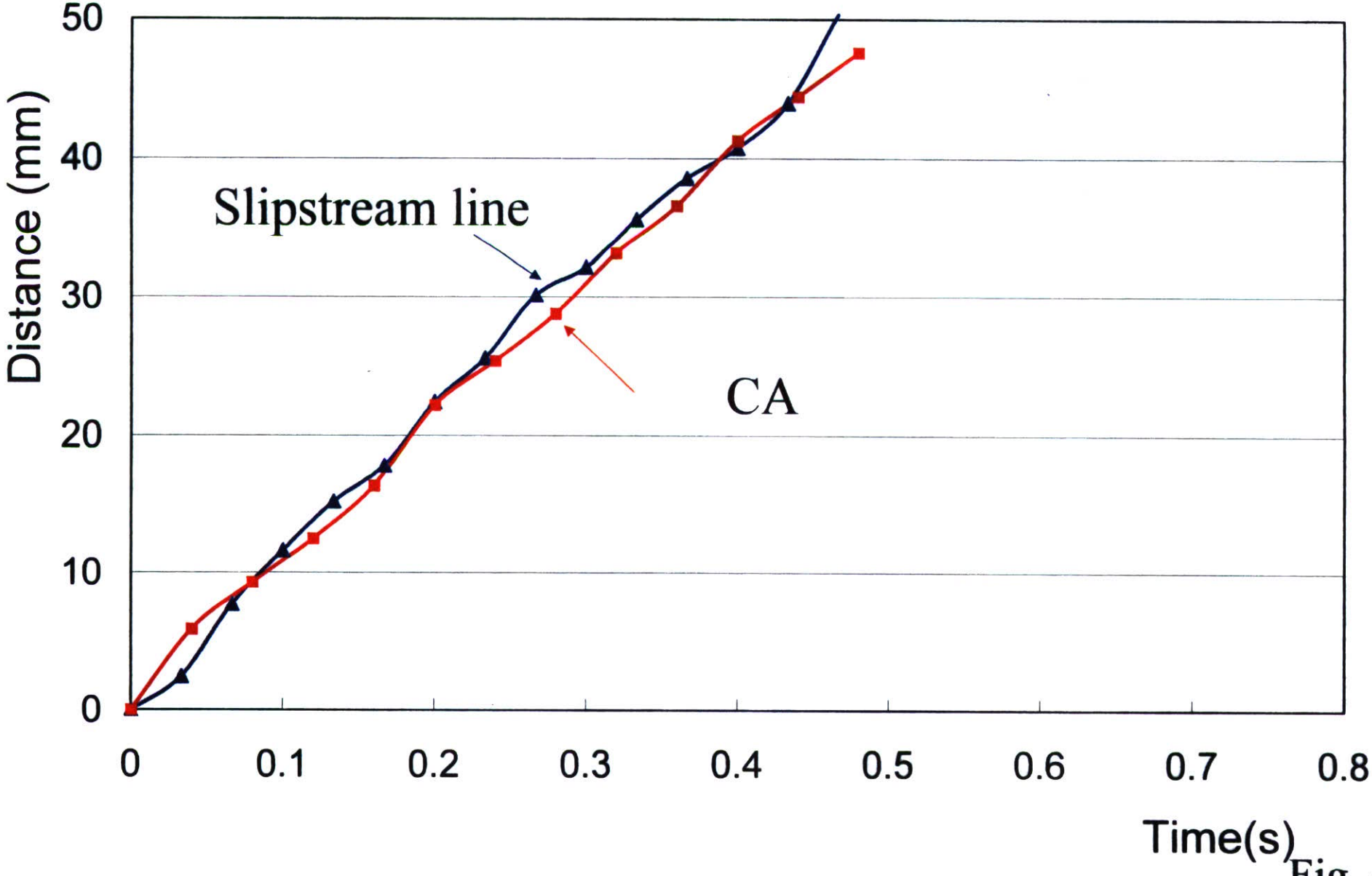
50
40
30
20
10
0
Distance (mm)
Slipstream line
CA
0
0.1
0.2
0.3
0.4
0.5
0.6
0.7
0.8
Time(s)

Fig. 4

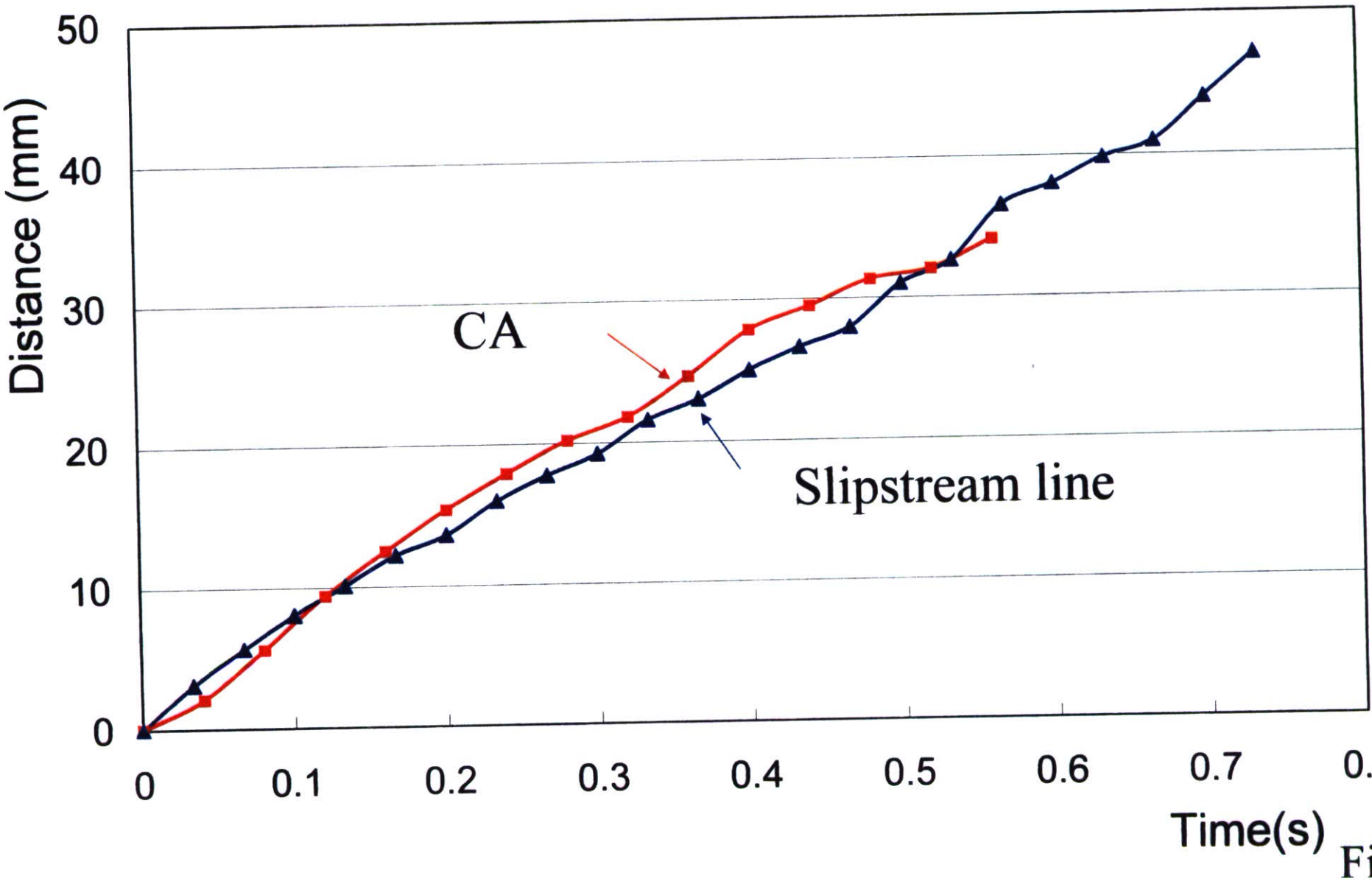
50
40
30
20
10
0
Distance (mm)
CA
Slipstream line
0
0.1
0.2
0.3
0.4
0.5
0.6
0.7
0.8
Time(s)

Fig. 5

	Without stent	With stent
Slipstream line (mm/s)	106.8±11.3	72.3±10.1
CA (mm/s)	109.6±13.7	70.9±7.7

Table 1

—Reviews—

細胞組織利用医療機器に用いられる幹細胞の品質及び安全性評価について

澤田留美,* 伊藤友実, 土屋利江

Safety Evaluation of Tissue Engineered Medical Devices Using Normal Human Mesenchymal Stem Cells

Rumi SAWADA,* Tomomi ITO, and Toshie TSUCHIYA
Division of Medical Devices, National Institute of Health Sciences, 1-18-1 Kamiyoga, Setagaya-ku, Tokyo 158-8501, Japan

(Received January 17, 2007)

Several recent studies demonstrated the potential of bioengineering using somatic stem cells in regenerative medicine. Adult human mesenchymal stem cells (hMSCs) derived from bone marrow have the pluripotency to differentiate into cells of mesodermal origin, *e.g.*, bone, cartilage, adipose, and muscle cells; they, therefore, have many potential clinical applications. On the other hand, stem cells possess a self-renewal capability similar to cancer cells. For safety evaluation of tissue engineered medical devices using normal hMSCs, in this study, we investigated the expression levels of several genes that affect cell proliferation in hMSCs during *in vitro* culture. We focused on the relationship between the hMSC proliferation and their transforming growth factor β (TGFβ) signaling during *in vitro* culture. The proliferation rate of hMSCs gradually decreased and cellular senescence was observed for about 3 months. The mRNA expressions of TGFβ1, TGFβ2, and TGFβ receptor type I (TGFβRI) in hMSCs increased with the length of cell culture. The mRNA expressions of Smad3 increased, but those of c-myc and nucleostemin decreased with the length hMSCs were in *in vitro* culture. In addition, the expression profiles of the genes which regulate cellular proliferation in hMSCs were significantly different from those of cancer cells. In conclusion, hMSCs derived from bone marrow seldom underwent spontaneous transformation during 1—2 months *in vitro* culture for use in clinical applications. In hMSCs as well as in epithelial cells, growth might be controlled by the TGFβ family signaling.

Key words——human mesenchymal stem cells; tissue engineered medical devices; proliferation; transforming growth factor β

1. はじめに

様々な疾病などに起因した組織や器官の機能不全に対して，組織再生又は機能回復を目指した「再生医療」が，現在注目されている．その手段としてこれまでに，幹細胞や人工素材を用いた医療機器の開発や細胞治療などについて多くの研究がなされている．胚性幹細胞（ES 細胞）は全能性を持つが受精卵を用いることから倫理的問題が大きいのに対し，体性幹細胞は ES 細胞のような倫理的問題がない点が再生医療や細胞治療のツールとして利用されている大きな理由であろう．中でも骨髄に含まれる間葉系幹細胞，造血幹細胞，血管内皮前駆細胞は，様々な臨床分野での応用が期待されている．また，骨髄や臍帯血中には間葉系幹細胞や造血幹細胞よりもさらに上の段階で多くの細胞系への分化能を持った細胞（multipotent adult progenitor cells; MAPCs）が存在することも報告されている.[1] さらに骨髄中だけでなくそれぞれの組織に特異的な幹細胞（肝，心筋，神経，上皮など）の存在も知られている．骨髄由来の間葉系幹細胞は骨，軟骨，脂肪，筋肉へ分化可能な細胞として広く知られている[1—5]が，さらに，神経細胞[3]や肝細胞,[1,6] 心筋,[7,8] 皮膚など胚を越えた分化も報告されており，整形外科の分野のみならず動脈硬化症，心筋梗塞，肝硬変，糖尿病などの治療への応用も期待されている．骨髄間葉系幹細胞は採取も比較的容易で *in vitro* での培養技術も確立されているため，細胞組織利用医療機器の材料と

国立医薬品食品衛生研究所療品部（〒158-8501 東京都世田谷区上用賀 1-18-1)
*e-mail: rsawada@nihs.go.jp
本総説は，日本薬学会第 126 年会シンポジウム S4 で発表したものを中心に記述したものである．

して最も実用に近いものの1つであろう．

しかしその反面，幹細胞は多分化能と同時に自己複製能を持つ細胞である[9]ため，正常細胞でありながら増殖能力を持つという点で癌細胞と共通の性質を持つともいえる．そのような背景の中，Rubioら[10]により脂肪組織由来のヒト間葉系幹細胞を長期間（4—5ヵ月）*in vitro* で培養すると自然に形質転換（癌化）するという報告がなされた．一方最近，間葉系幹細胞の由来によるその性質の違いについて，骨髄，臍帯血，脂肪組織由来の間葉系幹細胞をそれぞれ比較することによって示した報告[11]もあり，脂肪組織由来のヒト間葉系幹細胞が自然に形質転換するという上記の報告[10]が直ちに骨髄由来の間葉系幹細胞やさらには他の体性幹細胞も同様な変化を起こすということにはならないが，やはりその危険性に対して注意を払う必要はあるであろう．特に，体性幹細胞を細胞組織利用医療機器や細胞治療に用いるためには，生体内から取り出したのち *in vitro* で培養しある程度の細胞数を得なければならない．このため，少なくとも *in vitro* での培養中に幹細胞の性質ができるだけ変化しないことが望ましい．幹細胞を用いた細胞組織利用医療機器や細胞治療の実用化に向けて *in vitro* での培養中における幹細胞の安全性評価法の早期確立が重要課題であろう．

その第一歩として，筆者らは現在，幹細胞の *in vitro* での培養中に起こる遺伝子発現レベルの変化について検討を行っている．その理由としては，幹細胞におけるいくつかの遺伝子発現について調べることでその安全性を評価できる系を最終的に確立できれば，誰でも簡便に評価できるためであり，幹細胞を用いた細胞組織利用医療機器等の開発の促進につながることを期待している．本稿では，幹細胞の自己複製制御機構を探るために骨髄由来ヒト間葉系幹細胞の *in vitro* での培養中に起こる遺伝子発現レベルの変化について検討した結果を紹介する．

2. ヒト骨髄由来間葉系幹細胞の増殖能について

ヒト骨髄由来間葉系幹細胞（hMSC; Cambrex 社より2継代目の凍結細胞を購入）を *in vitro* で培養していくと，通常その増殖能は次第に低下していく（Fig. 1）．細胞を採取した個体による増殖速度の差はみられるものの，そのほとんどが培養期間2ヵ月を超えると増殖速度は低下し始め，4—5ヵ月になるとほとんど増殖しなくなってくる．増殖速度が低下した幹細胞は Senescence associated β-galactosidase（SA-β-Gal）staining によって細胞中に老化している細胞が含まれていることが確認された．増殖因子を添加した培地を用いた培養も行っているが，増殖速度は上昇するものの培養期間による速度の変化は増殖因子を加えていない細胞と同様であり，長期間培養しても無限増殖する幹細胞の存在は現在の所筆者らは確認していない．

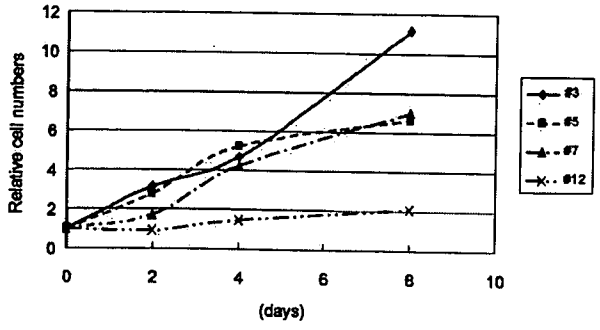

Fig. 1. Proliferation of hMSC in 3rd, 5th, 7th, and 12th Passages[16]

hMSC were seeded at 1.7×10^5 cells/Φ60 mm dish (6000 cells/cm^2), and cells were counted after 2, 4, and 8 days. The initial cell number (0 day) is expressed as 1, and the other cell numbers (2, 4, and 8 days) are relative to that of day 0. $n=3$.

3. *In vitro* 培養における hMSC の遺伝子発現レベルの変化について

上述したように，hMSC は *in vitro* での培養を続けることによってその増殖能は低下してくる．また細胞の形態等の変化もみられており，培養期間中に遺伝子の発現に変化が生じる可能性が示唆された．そこで，*in vitro* 培養期間の長さによる hMSC の遺伝子発現レベルの変化について調べるために，まず DNA アレイ解析（BD Atlas™ Human Cancer 1.2 Array）を行った．培養期間1ヵ月程度の細胞と2ヵ月以上の細胞とで比較検討した．それぞれの遺伝子の機能による分類単位での変化について Table 1 に示した．こちらはあくまで全体的な傾向を示しているため，それぞれの分類に含まれる個々の遺伝子の発現の変化がすべて同じという訳ではないが，hMSC は *in vitro* での培養を続けることによって遺伝子発現レベルの変化が起こることは確認された．hMSC の培養中に癌化といった形質転換が起こっていないことを確かめる指標を探るために「細胞増殖」という点に着目し，また上記の DNA アレイ解析結果も踏まえて，次に個々の遺伝子の発現レベル

Table 1. Comparison of Gene Expressions in hMSC (1 Month Culture) and hMSC (Over 2 Months)

The genes concerned with the following functions were up-regulated with the culture term
• Cell cycle
• Cell adhesion receptors/proteins
• Immune system proteins
• Oncogenes and tumor suppressors
• Stress response proteins
• DNA binding and chromatin proteins
• Cell receptors (by ligands)
• Cell receptors (by activities)
• Intracellular transducers/effectors/modulators
• DNA synthesis, recombination, and repair
The genes concerned with the following functions were down-regulated with the culture term
• Membrane channels and transporters
• Metabolism
• Translation
• Apoptosis associated proteins
• RNA processing, turnover, and transport
• Protein turnover
• Cytoskeleton/motility proteins

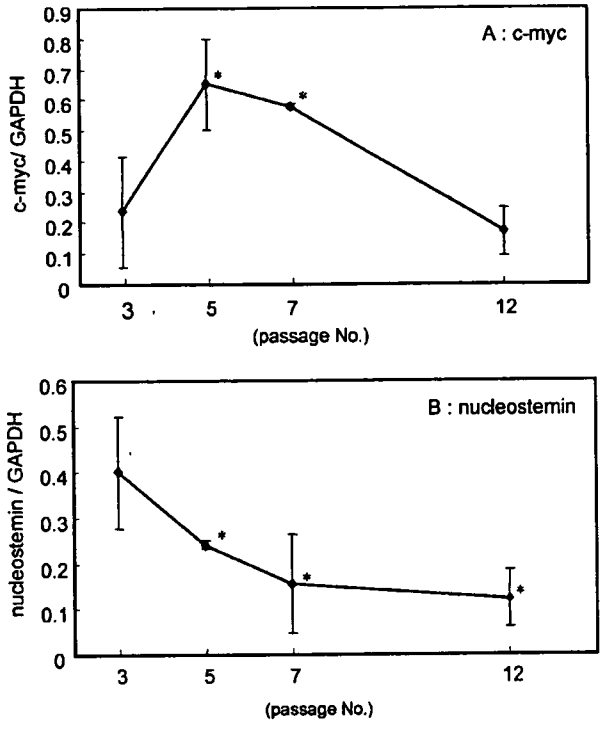

Fig. 2. Effect of *In vitro* Culture Length on the mRNA Expressions of c-myc (A) and Nucleostemin (B) in hMSC[16]

Expressions of the two genes relative to GAPDH in confluent cultures of hMSC in the 3rd, 5th, 7th, and 12th passages were investigated by quantitative RT-PCR. Mean values with standard deviations from three independent experiments are presented. Asterisks denote statistically significant differences compared with the 3rd passage ($*p<0.05$).

の変化について hMSC の培養期間を 4 点取り検討した．まず，癌遺伝子の 1 つであり細胞の増殖機能に係わる c-myc，幹細胞と癌細胞の両者の増殖に係わる nucleostemin，様々なシグナル伝達経路や発癌に係わるといわれている Wnt-8B について検討したところ，c-myc 及び nucleostemin (Fig. 2) は hMSC の培養期間の長さに依存してそれぞれの発現レベルは低下した．一方，Wnt-8B についてはどの培養期間においてもその発現は認められなかった．さらに，細胞増殖，分化，アポトーシス，細胞外マトリックス形成，免疫抑制そして発癌などの制御に係わる TGFβ について検討した．TGFβ には 3 つの分子種が存在 (TGFβ1, 2, 3) し，TGFβ は細胞表面にある 3 つのタイプの受容体 (TGFβRI, II, III) を通じてシグナルを細胞内へ伝達する．TGFβRI と TGFβRII はセリン-チロシンキナーゼで，TGFβRIII はベータグリカンとして知られている．[12] TGFβ はまず TGFβRII に直接か又は TGFβRIII を介して結合し，TGFβRII によって TGFβRI を刺激することで細胞内 TGFβ シグナル伝達系がスタートする．活性化された TGFβRI が Smad2 若しくは Smad3 をリン酸化したのち，シグナルを核内へと伝え c-myc のような TGFβ に依存する遺伝子の転写を制御する．[13,14] そのため，TGFβ の 3 種類の分子種と 3 タイプの受容体及び Smad3 についても hMSC の培養期間によるその発現レベルの変化について調べた．TGFβ1 及び TGFβ2 は *in vitro* での培養を続けることによってその発現レベルが上昇したが，TGFβ3 は変化しなかった (Fig. 3)．受容体についてはタイプ I は上昇したが，タイプ II 及び III は変化がみられなかった (Fig. 3)．Smad3 は TGFβ1, β2 及び TGFβRI と同様に上昇した．以上の結果から hMSC の培養中の遺伝子発現について，TGFβ→c-myc へのシグナル伝達系に係わる因子についての変化を Fig. 4 にまとめた．hMSC は *in vitro* での培養を続ける過程で，TGFβ→TGFβRI→Smad3→c-myc の経路で細胞周期停止が起こり，細胞の増殖が抑制されるのかもしれない．

以上の結果から，hMSC を *in vitro* で培養することによって通常はその増殖能が徐々に低下していき，その間の遺伝子発現の変化からも上皮系の他の

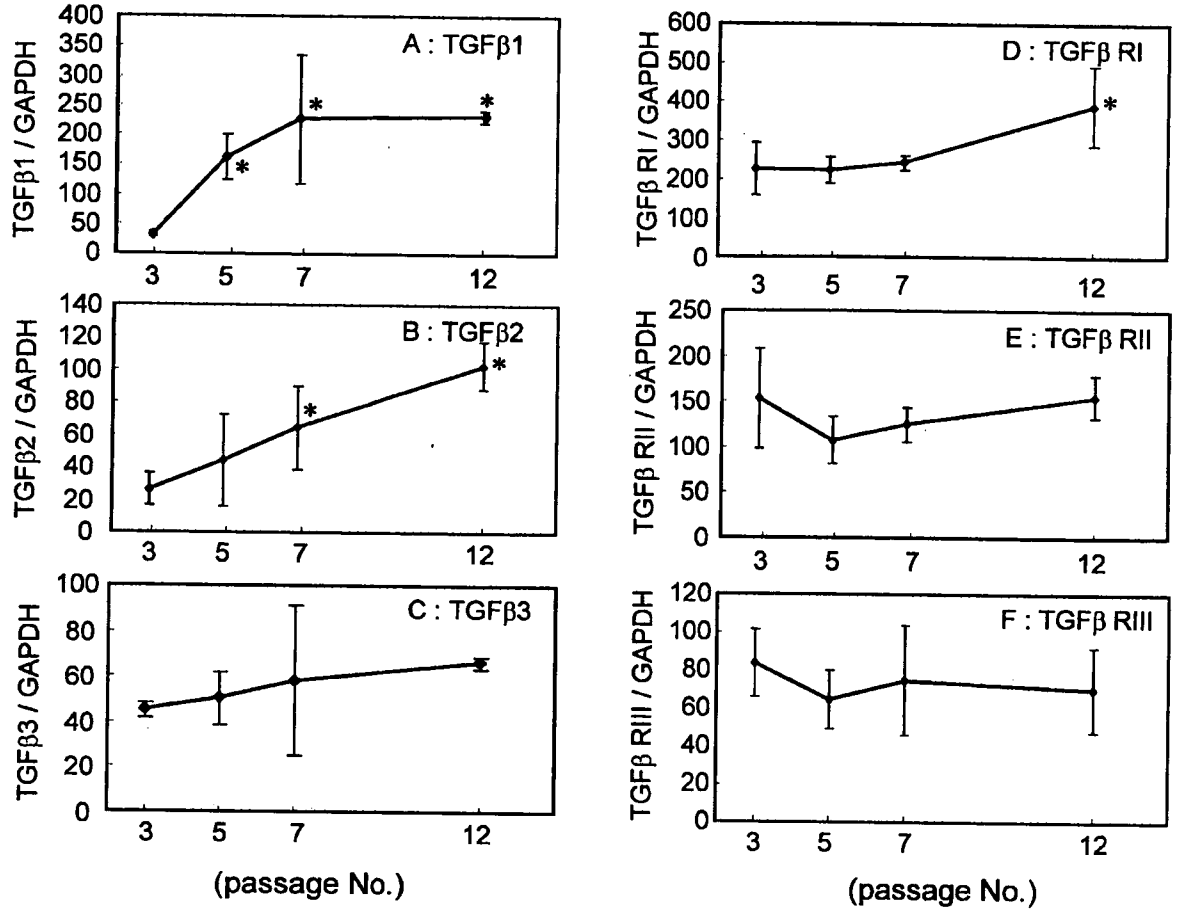

Fig. 3. Effect of *In vitro* Culture Length on mRNA Expressions of TGFβ1 (A), TGFβ2 (B), TGFβ3 (C), TGFβRI (D), TGFβRII (E), and TGFβRIII (F) in hMSC[16]

Expressions of the four genes, relative to GAPDH, in confluent cultures of hMSC in the 3rd, 5th, 7th, and 12th passages were investigated by quantitative real time RT-PCR. Mean values with standard deviations from three independent experiments are presented. Asterisks denote statistically significant differences compared with the 3rd passage ($*p<0.05$).

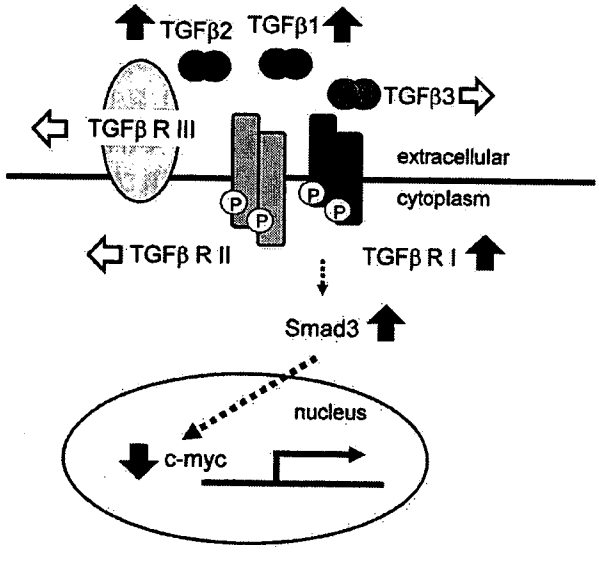

Fig. 4. Changes in the Expressions of TGFβ Signaling Genes during hMSC *In vitro* Culture for Three Months

細胞と同様なメカニズムで細胞増殖抑制が起こっていると考えられる．もしもこのような細胞の変化が「正常」な変化であると考えた場合，hMSC が培養中に形質転換等の望ましくない変化を起こした場合には違った発現パターンがみられる可能性があり，本研究で検討した遺伝子が幹細胞における培養中の変化に対する安全性評価の 1 つの指標となり得るかもしれない．現在，遺伝子発現の変化における hMSC の個体差を考慮し個体差を超えた共通性を見い出すために，複数の個体由来の hMSC を研究対象とし，また細胞の癌化や老化という観点からも更なる検討を行っている．

4. 幹細胞と癌細胞における遺伝子発現の比較について

幹細胞の癌化について，その危険性を評価するためには「自然に癌化した」幹細胞との比較検討が必